NASA TECHNICAL MEMORANDUM

NASA TM X-71504

NASA TM X-71504

AN AERODYNAMIC STUDY OF SCRAMJET FUEL INJECTORS

Louis A. Povinelli
Lewis Research Center
Cleveland, Ohio 44135

TECHNICAL PAPER proposed for presentation at Symposium on The Fluid Mechanics of Combustion sponsored by the American Society of Mechanical Engineers and the Canadian Society of Mechanical Engineering Montreal, Canada, May 13-16, 1974.

AN AERODYNAMIC STUDY OF SCRAMJET FUEL INJECTORS

Louis A. Povinelli
Aeronautical Research Scientist
Aerodynamic Analysis Section
NASA-Lewis Research Center
Cleveland, Ohio

E-7849

ABSTRACT

The aerodynamic drag and fuel distribution patterns of injectors designed for a supersonic combustion ramjet were measured at Mach numbers of 2, 2.5, and 3. The most significant parameter effecting the drag was found to be the injector thickness ratio. A two-fold reduction in the thickness ratio caused a 65 percent decrease in drag. Changing the injector sweep angle a factor of 2 resulted in only a small change in drag. A reversal of injector sweep, from sweepback to sweepforward, did not change the measured drag.

Helium gas was injected through the struts to simulate the penetration and spreading patterns of hydrogen. Sampling measurements were made at approximately 2 duct heights downstream of the combustor. The spacing required between fuel injectors was found to be about 10 jet diameters. The effect of gas injection on the measured drag was found to be minor.

NOMENCLATURE

b	chord fraction
C_D	drag coefficient
c	vertical spacing (see fig. 12)
D	drag
h	combustor height
L_1	combustor length (top and bottom plates)
L_2	combustor length (side plates)
ℓ	chord length
M	Mach number
P_0	total pressure
p	static pressure
q	dynamic pressure ($\frac{\gamma}{2} p_\infty M_\infty^2$)
r	leading edge radius

S strut span

s strut spacing (center-to-center)

T combustor thickness (top and bottom plates)

t strut thickness

w combustor width

x downstream (axial) direction

y vertical direction

z lateral direction

β Mach angle

γ specific heat ratio

δ thickness ratio (t/ℓ)

Λ sweep angle

Subscripts:

e plane normal to leading edge

ef effective

f friction

m mean

th thickness

1 strut root or leading edge or upstream

2 strut tip or trailing edge or downstream

∞ free stream

Superscript:

$\bar{}$ average

INTRODUCTION

Sustained atmospheric flight in the Mach 6 to 12 regime will require an advanced airbreathing propulsion system. The supersonic combustion ramjet (scramjet) has the potential for providing the propulsion at those flight velocities. Recent studies indicate that the scramjet powered vehicle provides best overall performance when the propulsion module is mounted as shown in fig. 1 (ref. (1)). This integrated design makes use of the underside of the vehicle, first to provide compression and secondly, to provide an expansion surface for the exhaust stream. The combustor section is relatively short in length and would have a means for hydrogen fuel injection. The hydrogen must react and burn completely prior to leaving the combustor. Only limited information is available for designing the fuel injectors. This study was performed to obtain relevant data for injector design. Specifically, fuel distribution patterns were obtained for various injector geometries. The drag of the injectors was also measured over a Mach 2 to 3 range corresponding to typical combustor inlet velocities. Testing was performed in a 0.31 m × 0.31 m (1 ft × 1 ft) wind tunnel at Reynolds numbers/meter of 7.8×10^6 to 35.1×10^6 (2.4×10^6 to 10.6×10^6 per foot).

APPARATUS AND PROCEDURE

Tunnel

Testing was performed at Mach 2, 2.5, and 3 in a 0.31 m × 0.31 m (nominal 1 ft × 1 ft) wind tunnel. Calibration and starting data are given in ref. (2). The total pressure of the air stream was varied from 100 to 276 kN/m^2 (14.5 to

40 psia) and the total temperature was 295 K (530 R). The dynamic pressure variation was from 37.9 to 48.3 kN/m^2 (792 to 1008 psfa). The Reynolds number/meter of the free stream varied from 7.8 to 35.1 million (2.4 to 10.6 million per foot).

Combustor Section

A simulated combustor section was installed in the test section of the tunnel. The rectangular cross-section was 22.85 cm (9 in.) high by 30.5 cm (12 in.) wide. The side plates were 40.8 cm (16 in.) long and were flush with the inside wall of the wind tunnel, fig. 2a. The top and bottom walls of the test section were 66.1 cm (26 in.) long and had a 15° wedge angle on the external leading and trailing edges. The combustor was mounted on 6 linear motion bearings which allowed it to move in the longitudinal direction of the tunnel. The motion was restrained by a load cell (444.8 N or 100 lb_f) as shown in fig. 2b. The housings which contained the linear bearings were mounted to a pressure box which in turn was fixed to the external tunnel wall. In this fashion, the load created by the combustor section and the struts could be measured. Further information on the drag suspension is given in ref. (2).

The fuel injector struts were mounted through the combustor section side plates (fig. 2b). Three injector ports were located on each side plate. The upstream port was located on the tunnel centerline and the two ports downstream were 7.63 cm (3 in.) apart, 3.82 cm (1.5 in.) from the center line. The longitudinal spacing between the two stations was 30.5 cm (12 in.).

Clearance between the combustor section and the tunnel walls was maintained at 0.051 cm (0.020 in.) as shown in fig. 2b. This clearance was also maintained between the extended portions of the top and bottom plates and the inside wall of the tunnel (refer to fig. 2b). The external pressure box eliminated the need for complicated seals between the moveable section and the tunnel walls.

The drag balance was calibrated by weights suspended from a pulley arrangement. Periodic calibration of the drag system was made throughout the testing program. The accuracy of the drag balance was ±2.2 N (±0.5 lb_f) over the load range.

Static pressure taps were installed along the centerline of the top and bottom plates of the combustor. Pressure taps were also placed on the bottom plate halfway between the tunnel side wall and the tunnel centerline.

Fuel Injectors

Nine different strut (fuel injector) geometries were selected for testing. The baseline or reference design was essentially that used by Metzler and Mertz (ref. (3)) in supersonic combustion testing, fig. 3. All of the struts were symmetrical double wedges and had sweepback. Each strut had 18 orifices located as shown in fig. 3. Six of the orifices were located on the ridge line on both sides of the struts. The remaining six orifices were located on the trailing edge of the strut. (Injection from the trailing edge was expected to yield a small amount of thrust thereby reducing the overall drag.) For some of the tests, an additional orifice was located in the tip of the strut as shown in fig. 3. The location of the orifices duplicates that of ref. (2) which was used in a cylindrical combustor. The modifications to the base line design (strut number 1) are shown in the table of fig. 3. Strut number 2 duplicates the basic strut but has a leading edge radius which is only one half as large. The trailing edge radii were the same for all struts ($r/\ell_1 = 0.005$). Strut number 3 has its maximum thickness at the 50 percent chord point. Struts 4 and 5 are reduced in thickness ratio ($\delta = t/\ell_1$) to 10 and 7.5 percent, respectively. Struts 6, 7, and 8 have less sweepback (Λ_1), and strut 9 is the same as 4 except it was reduced in length from 12.7 cm (5 in.) to 10.4 cm (4.1 in.). The thickness ratio was constant along the strut (root to tip) for all the geometries. The struts were fabricated as a shell from 16 gauge stainless steel (0.151 cm or 0.0595 in.). Four internal pins were welded into place inside the shell to provide support. This construction resulted in some surface waviness of the struts.

Fuel Injection and Distribution Measurements

Helium was used to simulate the injection of hydrogen. The amount of helium injected was varied in accordance with the mass flow of the airstream in order to obtain a stoichiometric fuel air mixture. The combustor section had a frontal area of 22.9 cm (9 in.) × 30.5 cm (12 in.) which amounts to 75 percent of the test section area. It was assumed that 3/4 of the air passed through the combustor. The helium flow rate was determined from measurements across an orifice plate. The injection pressure of the helium was adjusted so that the helium mass flow for the final strut configuration was 3 percent of the air flow. Prior to tunnel operation, internal strut pressure was measured. The flow through the injection orifices was found to be choked.

Samples were withdrawn from the flow stream using a wedge rake with 15 pitot probe tips. Each tip was made of 0.076 cm (0.030 in.) O.D. stainless tube with 0.0076 cm (0.003 in.) wall and protruded forward from the wedge a distance of 0.152 cm (0.06 in.). The center-to-center spacing of the probe tips was 0.508 cm (0.2 in.). The probe tips were connected to a 12 position scanning valve (rendering 3 randomly spaced tips inoperative). The probe is shown in fig. 2a, upstream of the combustor section. When taking gas samples, the probe was installed downstream of the combustor section and located on the tunnel side wall. The sampling rake was located at 1.72 combustor heights downstream of the trailing edge of the top and bottom plates ($x/h = 4.50$). The probe was mounted on an actuator mechanism on the side wall of the tunnel. Two mounting positions on the side wall were used; one on the tunnel center line, the other was located 6.99 cm (2.75 in.) above the tunnel center line. With these two positions it was possible to determine the presence of helium in approximately one half of the combustor.

The samples were continuously analyzed by a mass spectrometer for the amount of helium present in the sample. Sampling pressure was manually regulated to maintain a value of 20 mm Hg abs. The sampling system is described in ref. (4).

A helium manifold was installed inside the pressure box. Flexible tubing was used to connect the manifold to the struts. Calibration checks were made on the drag system to ensure that the manifold did not create a load on the combustor section.

RESULTS AND DISCUSSION

Pressure Distribution

The origin of the coordinate system used in this report and the static pressure distribution measured along the combustor section (in the absence of struts) are shown in fig. 4a. The measurements were made at the three values of the dynamic pressure shown on the figure. The upstream data are seen to scatter around the pressure ratio corresponding to Mach 2.5. A slight pressure rise is noted downstream ($x/h \approx 2$) at the top wall. The increase in pressure may have been partly caused by some waviness in the bottom plate of the combustor. Part of the pressure rise may also be due to the effect of skin friction. Fig. 4a shows the theoretical increase in pressure due to friction assuming an average friction coefficient of 0.0036. (The pressure rise due to friction was calculated assuming one-dimensional adiabatic flow.) This value of the coefficient was based on the drag measurements presented in the next section. The variation in static pressure was 0.1 to 0.2 psi and the accuracy of the pressure measurements was 0.1 psi. The observed difference between the calculated and measured rise in pressure may be attributable to the inaccuracies of the pressure measurements.

The static pressure distribution, measured with two struts located at the upstream station (one strut on each side of the combustor) is shown in fig. 4b. The shock waves due to the presence of the struts caused a two fold rise in static pressure at the rearward section of the combustor, both at the top and bottom walls. For reference purposes the data with no struts are also shown in the figure. The pressure distribution was also measured with six struts installed in the combustor (as shown in fig. 2a). The resulting distribution was

identical to that shown in fig. 4b. The shock waves caused by the four (downstream) struts, evidently, intersected the tunnel wall downstream of the combustor section. Hence the measured pressure distribution along the combustor section walls was determined by the upstream struts only.

The pressure distribution was also measured while helium was injected through the strut injectors. Peak pressures were observed to be slightly higher with helium injection.

Skin Friction Drag

The measured drag of the combustor with no struts is shown in fig. 5. This drag is due to the effect of skin friction and to the plate thickness (0.64 cm or 0.25 in.). Both the top and bottom plates of the combustor are immersed in the flow stream and contribute to thickness drag. The thickness (pressure) drag may be calculated using the following expression for the drag coefficient:

$$C_{D,th} = 2\delta^2 \Big/ \sqrt{M_\infty^2 - 1}$$

where $\delta = (T/L_1)_{plate}$. Substituting yields:

$$C_{D,th} = 8.73(10)^{-5}$$

The thickness drag may be calculated from:

$$D_{th} = \frac{\gamma}{2} p_\infty M_\infty^2 C_{D,th} L_1 w$$

where L_1 is the length of the top or bottom wall of the combustor (66.1 cm or 26 in.) and w is the width (31 cm or 12.2 in.). The resulting values for thickness drag are as follows:

Dynamic pressure, q		Drag, D	
kN/m^2	(lbs/ft^2 abs)	N	(lbs_f)
37.9	(792)	1.33	(0.30)
43.4	(907)	1.53	(0.34)
48.3	(1008)	1.70	(0.38)

The calculated thickness drag values are seen to be very small and may be neglected. The drag data shown in fig. 5, therefore, may be considered to be due to the effect of skin friction alone. In order to evaluate an average skin friction coefficient, we write:

$$\bar{C}_f = D_f/q(4L_1w + 2hL_2)$$

where the wetted area is $(4L_1w + 2hL_2)$. Evaluating the above equation at the three q values yields an average friction coefficient:

$$\bar{C}_f = 0.0036$$

Using this value of $\bar{C}_f$ to calculate drag gives the line shown in fig. 5.

Strut Drag

Reference strut drag

The drag of the combustor module with 6 struts (number 1 shown in fig. 3) was measured at Mach 2.5 at three dynamic pressure conditions. The result is shown in fig. 6. The addition of six struts increased the drag 190 N (43 lbs_f)

at the lowest pressure condition. The drag per strut amounts to about 32 N (7 lbs_f). At the highest dynamic pressure, 48 kN/m^2, the drag increased 245 N (55 lbs_f) which is approximately 41 N (9 lbs_f) per strut. Drag measurements were also made with only 2 struts installed in the module. The drag caused by the two struts mounted upstream was 66.7 N (15 lbs_f), 73.4 N (16.5 lbs_f) and 80 N (18 lbs_f) at the three dynamic stream conditions. The drag per strut again amounted to approximately 33 N (7 lbs_f), 37 N (8 lbs_f) and 40 N (9 lbs_f). The strut drag appears, therefore to be linearly dependent on the number of struts.

Drag measurements were also made with only 2 struts installed at the rearward station. The results are shown in fig. 6. The drag values are very close for both cases. Installation of the struts at the forward station caused shock wave intersection at the module wall (as seen in previous static pressure distribution in fig. 4b). The rearward installation caused the shock waves to fall outside (downstream) of the combustor section. The fact that the drag was the same with either forward or rearward mounting indicates that the shock wave - boundary layer interactions did not significantly alter the skin friction drag.

Effect of leading edge radius (r/L) and maximum thickness position (b). The effect of leading edge radius on drag was determined by comparison of strut number 1 with strut number 2. The radius-to-root chord ratio was 0.005 compared to 0.010 for strut number 1. Fig. 7 shows that the change in radius did not significantly (~1%) affect the measured drag. The effect of changing the position of maximum strut thickness also did not cause any noticeable alteration in the drag measurements. Strut number 3 had its maximum thickness at the 50 percent chord position compared to 70 percent for strut number 2. Measured drag values were the same. Within the range of the variables tested, therefore, the position of maximum thickness and the leading edge radius do not influence the drag force.

Thickness ratio (t/ℓ_1). Strut numbers 3, 4, and 5 were tested to determine the effect of thickness ratio on drag. The strut drag is shown in fig. 8 for the three struts. The contribution of the empty combustor section has been subtracted from the total drag values measured. Reducing the thickness ratio from 0.16 to 0.10 resulted in approximately a 50 percent drag reduction over the entire dynamic pressure range. A further reduction in thickness ratio (from 0.16 to 0.075) resulted in a 60 to 65 percent reduction over the same q range. These results show that the drag per strut ($q = 43.5\ kN/m^2$) for the 0.10 thickness geometry is about 17.8 N (4 lb_f). This value compares with 35.6 N (8 lb_f) for the 0.16 thickness strut. Therefore, it is possible to reduce combustor drag with use of the thinner struts. For example, using 8 to 10 of the 0.10 thickness ratio struts (depending on spacing requirements for proper fuel distribution) gives a drag of 142.4 N (32 lb_f) to 178 N (40 lb_f). With 6 struts, having 0.16 thickness ratio, the drag is 213.6 N (48 lb_f). These numbers represent a drag reduction of 17 to 33 percent.

To explain the trend of the data, calculations are made using linear theory. In accordance with linear wing theory, the drag coefficient at zero lift for a double wedge symmetrical airfoil is

$$C_D = \frac{4 \cos^3\Lambda \delta_e^2}{\sqrt{M_\infty^2 \cos^2\Lambda - 1}}$$

where δ_e is the thickness drag normal to the leading edge and the drag is:

$$D_{th} = \frac{4 q_\infty \cos \Lambda \delta^2}{\sqrt{M_\infty^2 \cos^2\Lambda - 1}} \ell S$$

Referring to the above equation, it may be seen that for fixed values of the dynamic pressure (q_∞), sweepback (Λ), chord length (ℓ), strut span (S), and Mach number the drag is proportional to the thickness ratio squared. Fig. 9 is a plot of the experimental strut drag versus thickness ratio squared with free stream dynamic pressure as a parameter. At the higher dynamic pressure values

the drag is nearly linear with δ^2 whereas at the lower dynamic pressure greater deviation is observed. The calculated drag, based on linear wing theory, is in reasonable agreement for the strut with low thickness ratio (δ of 0.075) but is a factor of 2 to 3 higher for the 10 and 16 percent struts. The lack of agreement may be due to the fact that linear theory becomes invalid for large perturbations. Also the finite span of the wing and the effect of strut taper affect the calculations. Struts 3, 4, and 5 have thickness ratios, δ_e, of 15, 20, and 32 percent.

Sweep of leading edge (Λ_1). Reduced sweepback is desirable so as to increase the residence time for the fuel. (Reducing sweepback may be undesirable with respect to thermal choking and leading edge cooling. Neither of these effects are considered in this report.) The effect of reducing sweepback on drag was measured using struts 6. 7, and 8. An attempt was made to optimize the strut design using the theoretical results of Puckett (ref. (5)). The three struts were designed with a constant value of sweepback angle to Mach angle ($\Lambda/\beta = 0.6$). The 36°, 40°, and 43° struts were designed for testing at Mach 2, 2.5, and 3 respectively. Testing was extended, however, for a given strut to all three Mach numbers. Typical results are shown in fig. 10 for a sweep angle of 40°. It was found that with all of the struts tested at the three Mach numbers and the range of dynamic pressures that a small drag increase occurred. Comparison of the strut drag data in fig. 10 with those for the 60° sweepback in fig. 8 ($\delta = 0.1$) shows a maximum increase in strut drag of 26.7 N (6 lbs_f). (Note that fig. 8 is a plot of strut drag only, whereas fig. 10 is a plot of strut and combustor drag.) Over the range of conditions investigated, the increased drag varied from only 1.80 to 4.45 N (0.40 to 1 lbs_f) per strut. The increase in drag, of approximately 25 percent for a 20° change in sweep angle, is in agreement with the data of Vincenti (ref. (6)).

Reversed sweep. Vincenti (ref. (6)) has also shown that the minimum pressure (thickness) drag of a swept wing is nearly unchanged by a reversal of the sweep. If this were the case for internal flows it would mean a further increase in fuel residence time within the combustor. (It is noted that reverse sweep may adversely affect inlet performance if the struts protrude upstream of the combustor entrance. The acute angle at the wall may also cause localized boundary layer separation and severe local heating rates. These effects remain to be studied.) Therefore, strut array number 5 was reversed so that the injectors pointed upstream. Since the trailing edge angle (Λ_2) was 40°, reversing the struts yielded a sweep angle of -50°. The difference in sweepforward and sweepback was 10° (i.e., -50 versus +60). The experimental data of Vincenti (ref. (6)) shows that changing the sweep angle from 60 to -50 will result in a 25 percent increase in the drag coefficient. The results of this study are shown in fig. 11. The sweptforward struts yielded 12, 18, and 24 percent greater drag than the sweptback struts at dynamic pressures of 37.9, 43.4, and 48.3 kN/m^2 respectively (792, 907, 1008 psfa). These results are in agreement with the expected increase in the drag coefficient based on ref. (6). It is concluded that struts with 60° forward sweep would yield virtually the same drag as 60° sweepback and would contribute substantially to the residence time of the fuel in the combustor. (It should also be noted that the trailing edge orifices were soldered closed when the blades were swept upstream. The orifices were closed so as not to cause strong local disturbances along the edge of the strut.)

Strut length. The sum of the thickness drag and skin friction drag is given by the expression:

$$D = 2\ell S q_\infty \left[\frac{2 \cos \Lambda \delta^2}{\sqrt{M_\infty^2 \cos^2 \Lambda - 1}} + \bar{C}_f \right]$$

For constant values of the dynamic pressure (q_∞), sweepback (Λ), thickness ratio (δ), Mach number (M_∞), and friction coefficient ($\bar{C}_f$), the drag is proportional to the planform area of the struts. The span of strut number 9 was 10.4 cm (4.1 in.) compared to 12.7 cm (5 in.) for strut number 4. The reduction in planform area between the two struts is 12.9 percent. The drag of struts number 9 were measured at Mach 2.5 and found to be lower than struts

number 4. The reduction in drag at a dynamic pressure value of 48 kN/m^2 was 7 percent and at 43 kN/m^2, the reduction was 8 percent. The magnitude of the strut drag being measured was about 111 N (25 lbs_f). The accuracy of the drag balance was ±2.23 N (±1/2 lb_f) which amounts to 4 percent of the measurement. Hence, the difference between the calculated decrease (12.9 percent) and the measured decrease may be attributable to the inaccuracy of the drag system and/or finite span or strut taper effects. It was concluded that the decreased drag is proportional to the change in strut length.

Distribution of Injectant

Sampling measurements showed that helium injected from the struts on one side of the combustor did not reach the (lateral) tunnel centerline. It was therefore assumed that lateral symmetry existed in the test section and sampling was carried out over half the tunnel width. Injection was made through three struts only. This procedure also reduced the quantity of helium required for testing.

Three different strut geometries were used in the sampling tests, namely numbers 2, 5, and 8. The center-to-center strut spacing (s in fig. 12) was fixed at 3.81 cm (1.5 in.). The minimum vertical distance (c in fig. 12) between the strut surfaces varied with the thickness ratio of the struts. The minimum vertical distance between the strut surfaces occurred at the ridge line of the struts and (due to strut taper) varied from the strut root to the strut tip. The vertical distances are given in the following table;

VERTICAL STRUT SPACING (c in fig. 12)

Strut number	Root	Tip
2	1.27 cm (0.50 in.)	2.44 (0.96)
5	2.24 cm (0.88 in.)	2.95 (1.16)
8	2.64 cm (1.04 in.)	3.15 (1.24)

Fig. 12 shows the concentration results obtained with struts number 8 in a Mach 3.0 airstream. The particular results shown are for a fixed lateral position in the stream ($z/h = 0.222$) and a fixed downstream position of 1.72 combustor heights ($x/h = 4.50$). The mass flow ratio of helium to air was 0.021. The relative strut positions are also shown in the figure. It is seen from these results that the concentration between the struts falls to nearly zero, indicating that very little helium has spread out and filled that region. The diameter of the orifices was 0.36 cm (0.141 in.). The injection pressure of the helium was increased to obtain greater penetration. However, the void regions still remained. The higher injection pressure corresponded to He/air ratios of 0.07. Results at other lateral positions showed the same qualitative behavior.

Results with strut number 5 are shown in fig. 13 for various lateral stream positions. The He/air ratio was 0.032 and the injection differed from the previous case in one manner. That is, the 6 trailing edge orifices were plugged so that all the helium was injected along the ridge line. With this arrangement the orifices were barely choked. The result is not significantly different from that obtained previously. An obvious void region still exists between adjacent struts. Increasing the injection pressure did not alter the results nor did a lowering of free stream Mach number (2.5). Use of smaller diameter orifices to ensure choked flow (0.132 cm diam or 0.052 in.) also did not change the observed behavior.

The results with struts number 2 are shown in fig. 14 for two He/air ratios. It may be seen that relative concentration between the struts is approximately 45 percent. The reduction in strut spacing (dimension c), in going from strut 8 to 2, has been sufficient to yield desirable spreading in the distance available. Increasing the He/air ratio does not appreciably alter the qualitative behavior. These tests were also run with struts having no trailing edge orifices. This particular strut array was probed in some detail and is shown in fig. 15 for various lateral stream positions. Fig. 15a shows distributions near the strut root and fig. 15b near the strut tip. It may be

seen that the helium distribution depends strongly on the lateral position. Also, sampling directly downstream of an orifice will yield high helium concentrations. The orifice spacing along the strut may be somewhat larger (10.8 to 17.7 jet diameters) than needed.

The final strut modification was to redrill the trailing edge orifices halfway between the ridge orifices and to drill one injection hole on the strut tip (see fig. 3 for tip hole location). All of the orifices were 0.132 cm diameter (0.052 in.). Detailed sampling was carried out with measurements being made at 0.635 cm (0.25 in.) intervals in the lateral direction, z, and at 0.508 cm (0.20 in.) intervals in the vertical direction, y. The downstream location was constant ($x/h = 4.50$). Contours of the concentration were plotted in fig. 16. Superimposed on the concentration contours are the projections of the two downstream struts and the upstream strut. In general, low concentrations of helium ($\leq$50 percent) were found downstream of the middle strut. The higher concentration regions ($\leq$95 percent) appeared downstream of the upper and lower struts. Since the helium injected upstream had a longer residence time in the combustor, more mixing occurred, leading to lower concentration levels at the sampling station. Several small regions of high concentration are seen between the upper and middle struts and may be associated with nonuniform flow turning. In general, the helium was distributed over the entire flow area. Further strut refinements such as a reduction in the orifice spacing (e.g., 6 to 10 jet diameters) may improve the distribution.

The concentration contours shown in fig. 16 were computer generated using a FORTRAN subroutine for contour plotting. This subroutine was used in conjunction with a bivariate interpolation method and smooth surface fitting based on local procedures. The programming was carried out by Mr. John Riehl of the Lewis Research Center.

Influence of Helium Injection on Drag Measurements

Drag measurements with the final strut modification (described in the previous section) were made both with and without helium injection. Injection was made through only three struts, using half the helium required for a stoichiometric mixture. At dynamic pressure of about 38 kN/m^2 (790 psfa), the decrease in drag with injection was 8.9 N (2 lbs_f) or approximately 3 N (0.66 lb_f) per strut. This drag reduction represents about 6 percent of the total drag as shown in fig. 7. For struts with low thickness ratios ($t/\ell = 0.075$ to 0.10), the measured reduction would be 8 to 9 percent (based on the drag values shown in fig. 8).

No drag decrease due to injection was noted for those struts tested without trailing edge injection. In fact, injection through the ridge orifices only, showed an increase in overall drag which was comparable to the accuracy of the drag balance ($\pm$2.2 N or $\pm$0.5 lb_f).

Conclusions

The drag of a rectangular scramjet combustion module having six swept injector struts was measured at Mach 2, 2.5, and 3. The dynamic pressure was varied from 37.9 to 48.3 kN/m^2 (792 to 1008 psfa) and the freestream Reynolds number per meter varied from 35.1×10^6 to 7.8×10^6 (10.6×10^6 to 2.4×10^6 per foot). The contribution of the combustor, without struts, to the drag (i.e., skin friction drag) was also measured. At Mach 2.5 the average friction coefficient was 0.0036.

The effect of the following variables on strut drag were investigated:
leading edge radius
position of maximum thickness
thickness ratio
sweep angle
strut length

Among these variables, thickness ratio was found to be the most significant. Reducing thickness ratio from 0.16 to 0.10 caused a 50 percent decrease in drag over the entire dynamic pressure range. The major significance of these results is that the use of a larger number of thin struts rather than

thick struts should result in lower overall drag. The greater number of thinner struts would also be helpful in obtaining uniform fuel distribution. The leading edge radius change (r/ℓ_1 from 0.005 to 0.01) and the position of maximum thickness (b from 0.5 to 0.7) did not significantly affect the drag measurements. A decrease in sweepback angle (Λ_1 of 60, 43, 40, and 36) caused a small increase in strut drag. This result is of interest since reduced sweepback offers the potential of more time for fuel mixing within the combustor. A complete reversal of the sweep, i.e., sweepforward rather than sweepback, did not significantly affect the drag measurements. Since forward sweep greatly increases combustor residence time, better overall fuel-air mixing could take place with this strut arrangement.

Measurements of the helium concentration were made at a fixed downstream station of 1.72 combustor heights for a fixed strut center-to-center spacing. The results showed that the spacing between strut surfaces had to be of the order of 10 jet diameters apart in order to obtain a reasonable concentration level between struts.

Helium injection at a mass equivalence ratio of unity and a freestream Mach number of 2.5 was found to reduce the total combustor drag by 6 to 9 percent.

REFERENCES

1 Henry, J. R., and Anderson, G. Y., "Design Considerations for the Airframe-Integrated Scramjet," The First International Symposium on Airbreathing Engines, Marseille, France, June 19-23, 1972.

2 Povinelli, L. A., Aerodynamic Drag and Fuel Spreading Measurements in a Simulated Scramjet Combustion Module, NASA TN D, to be published.

3 Metzler, A. J., and Mertz, T. W., " Preliminary Results of Large Supersonic Burning Combustor Testing," Journal of Aircraft, Vol. 9, No. 1, Jan. 1972, pp. 23-30.

4 Povinelli, L. A., Povinelli, F. P., and Hersch, M., "A Study of Helium Penetration and Spreading in a Mach 2 Airstream Using a Delta Wing Injector," NASA TN D-5322, July 1969.

5 Puckett, A. E., "Supersonic Wave Drag of Thin Airfoils," Journal of the Aeronautical Sciences, Vol. 13, No. 9, 1946, pp. 475-484.

6 Vincenti, W. G., "Comparison Between Theory and Experiment for Wings at Supersonic Speeds," NACA TN 2100, June 1950.

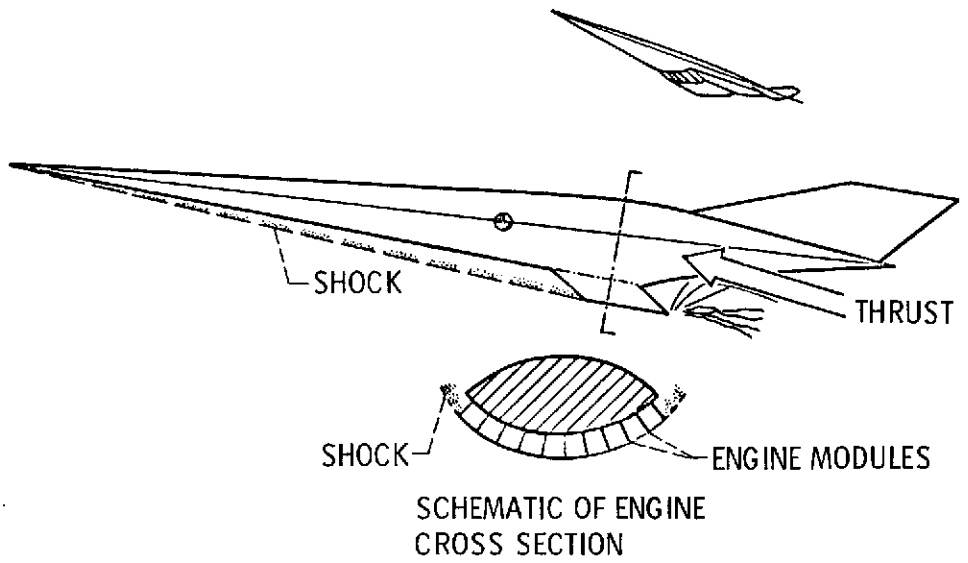

E-7849

Figure 1. - Scramjet-vehicle integration. (From ref. 1)

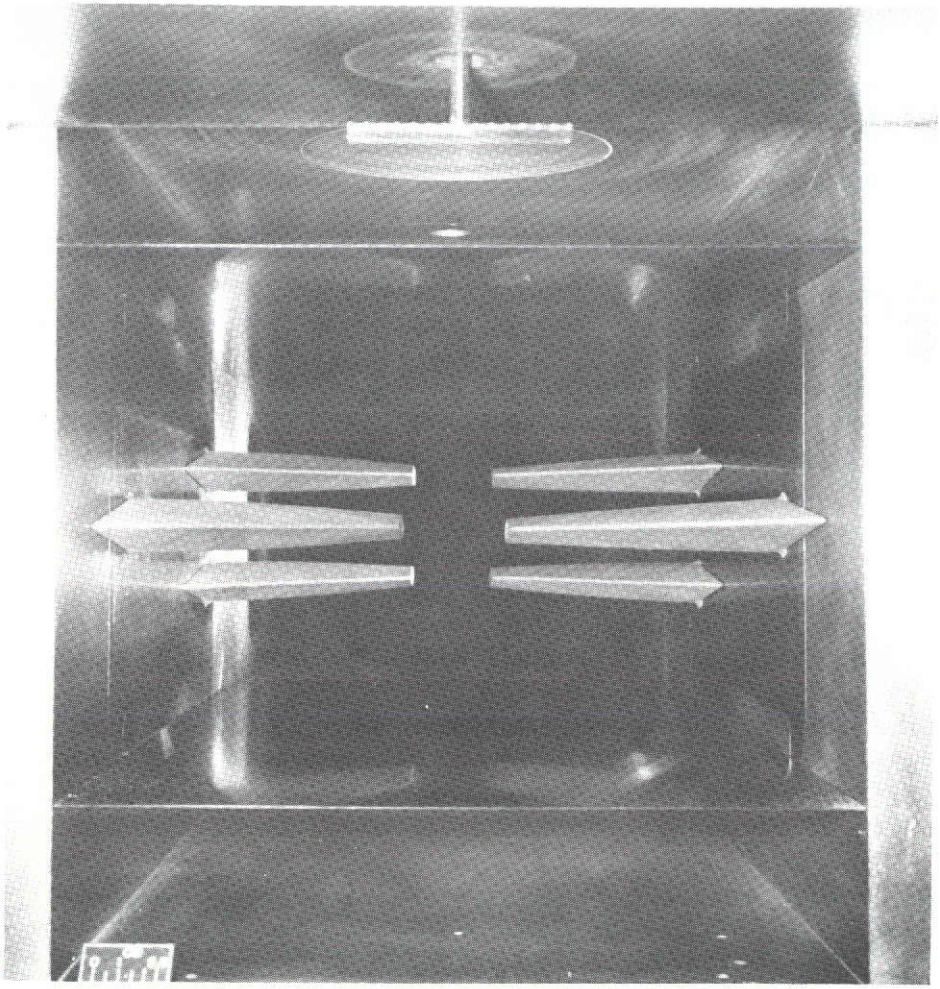

(a) Tunnel installation with number 1 struts. (Downstream view)

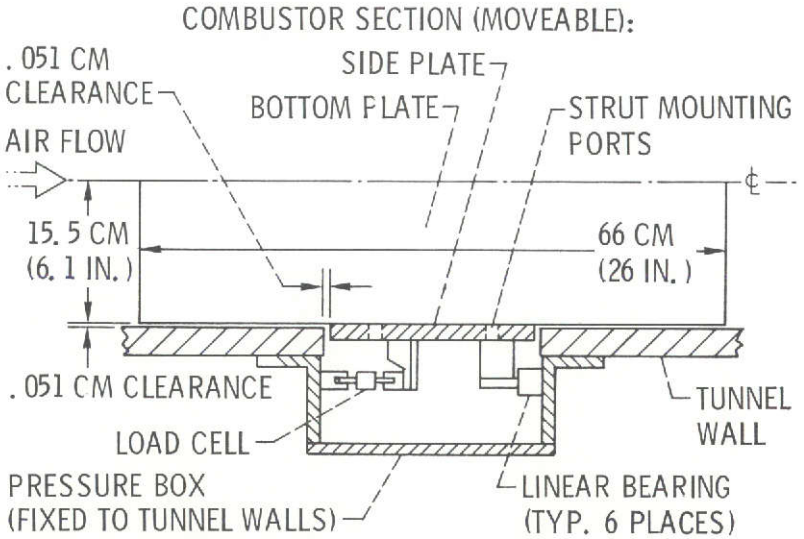

(b) Plan view of combustor installation in wind tunnel.

Figure 2. - Simulated combustor module.

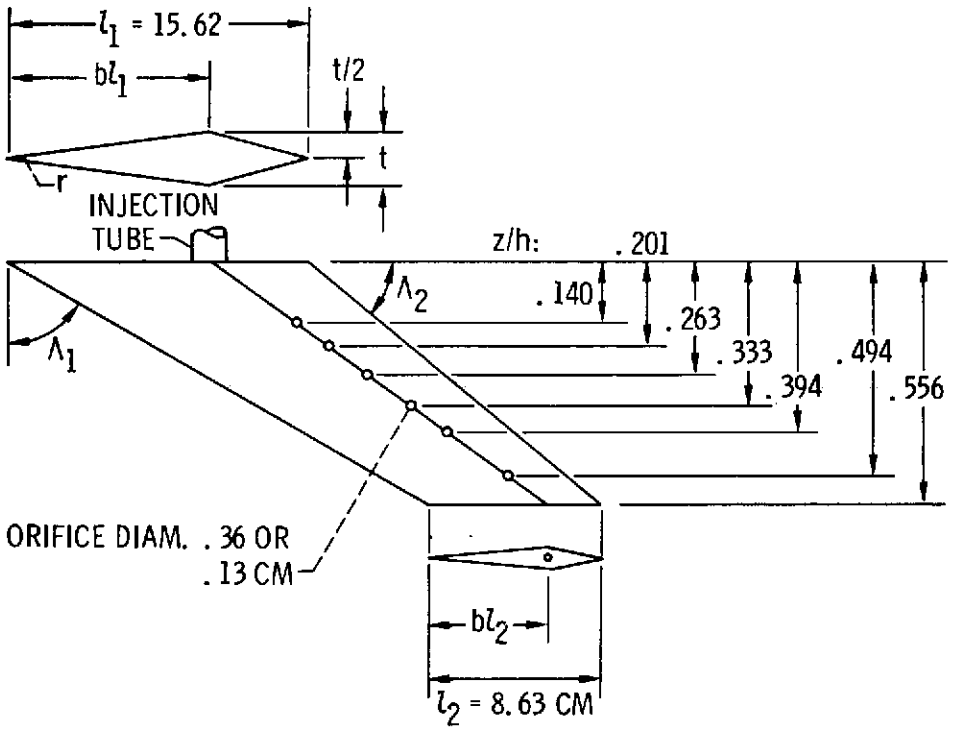

STRUT NO.	r/l_1	Λ_1	Λ_2	b	t/l
1	0.010	60^0	40^0	0.7	0.16
2	.005	60	40	.7	.16
3	.005	60	40	.5	.16
4	.005	60	40	.5	.10
5	.005	60	40	.5	.075
6	.005	36	80	.5	.10
7	.005	40	74	.5	.10
8	.005	43	69	.5	.10
9*	.005	60	40	.5	.10

*STRUT LENGTH REDUCED TO 10.4 CM FROM 12.7 CM.

Figure 3. - Injection strut geometries.

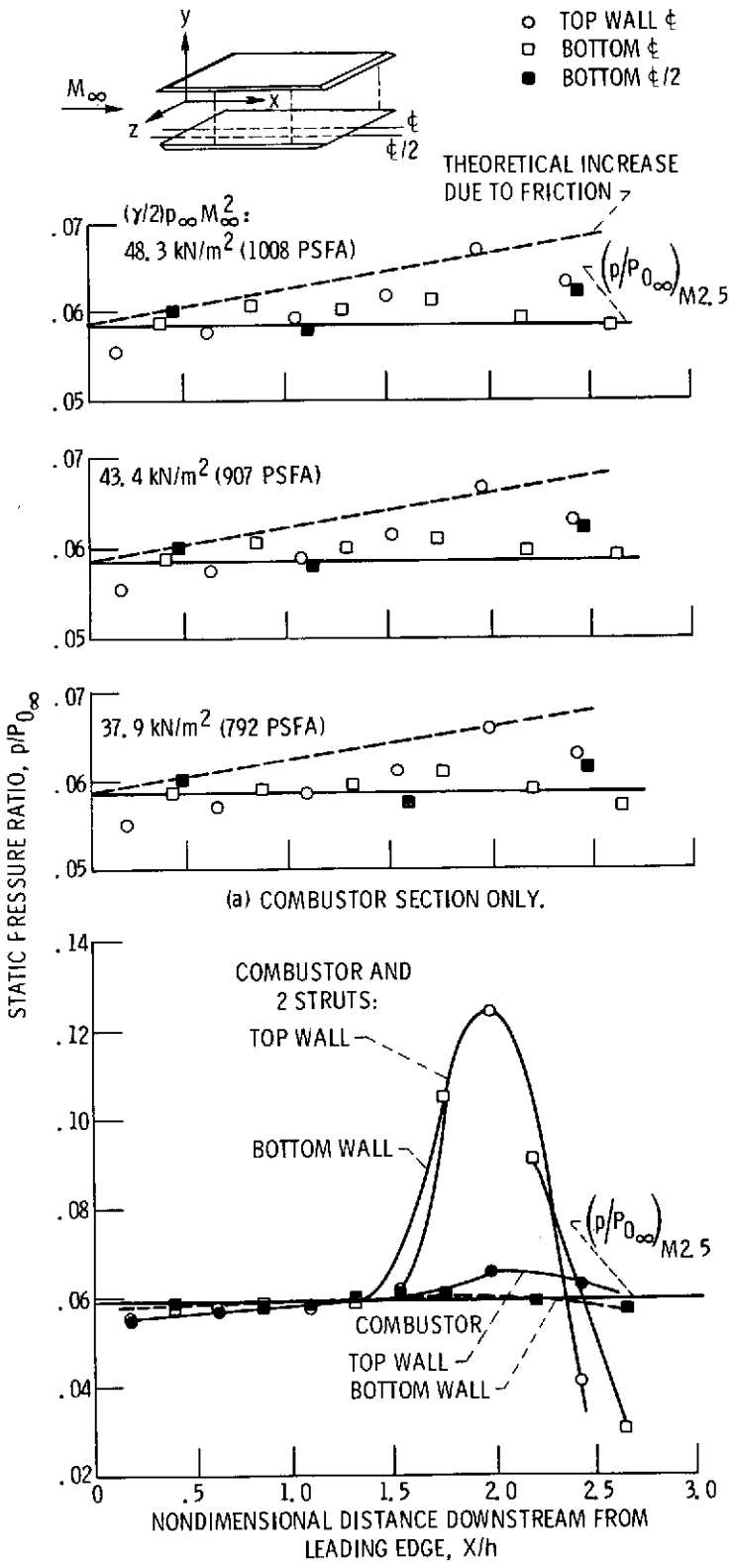

(b) COMBUSTOR AND STRUTS (2 NUMBER 1 STRUTS)
$\frac{\gamma}{2} p_\infty M_\infty^2$ = 37.9 kN/m^2 (792 PSFA).

Figure 4. - Static pressure distribution, Mach 2.5.

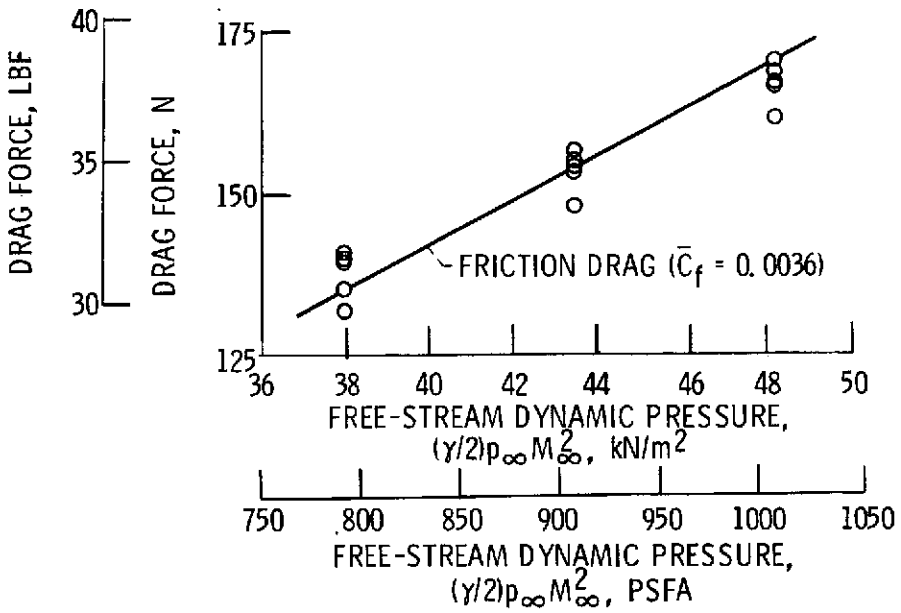

Figure 5. - Combustor section drag measurement (no struts), Mach 2.5.

E-7849

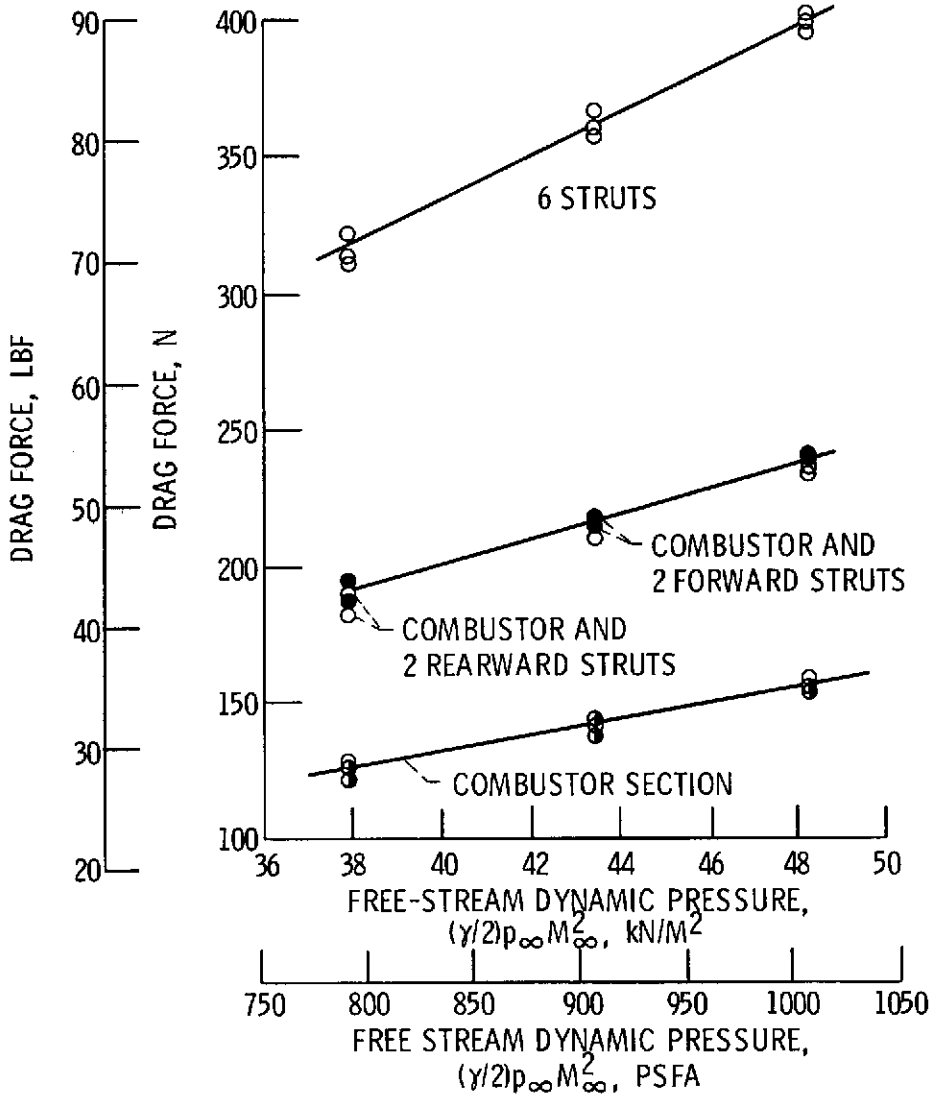

Figure 6. - Drag of combustor module with struts (number 1). Mach 2.5.

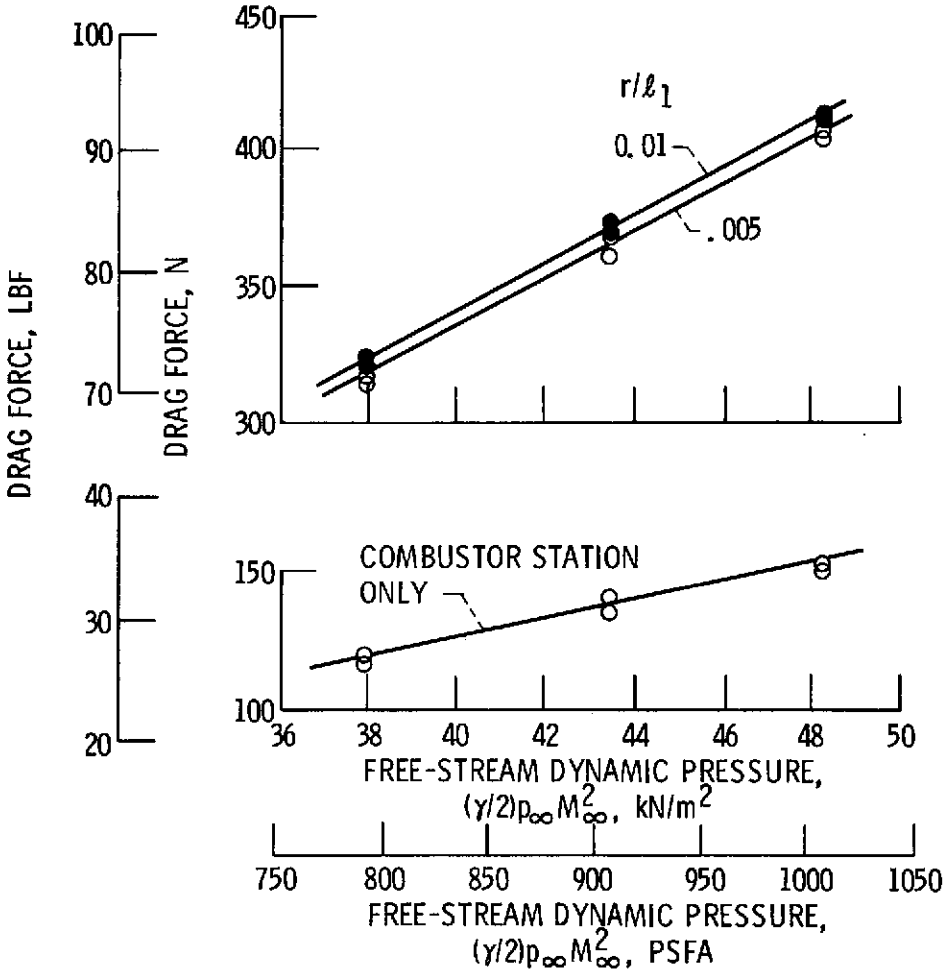

Figure 7. - Effect of leading edge radius on drag, Mach 2.5, six strut array.

E-7649

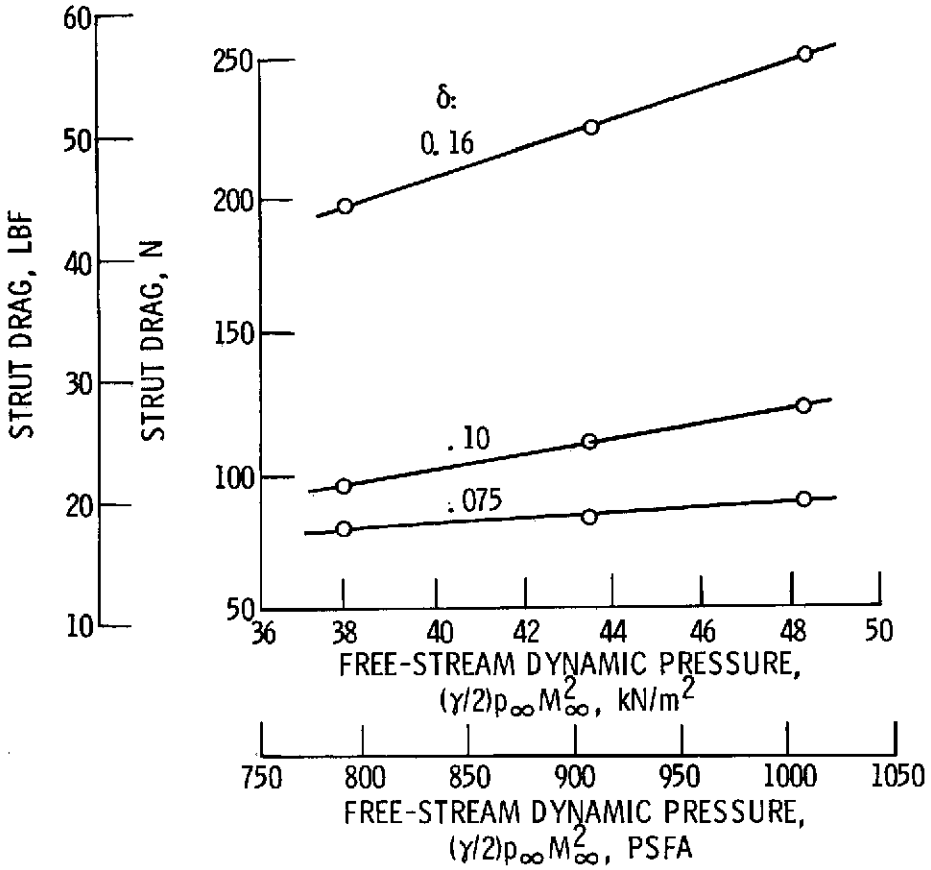

Figure 8. - Effect of strut thickness on drag, Mach 2.5, six strut array.

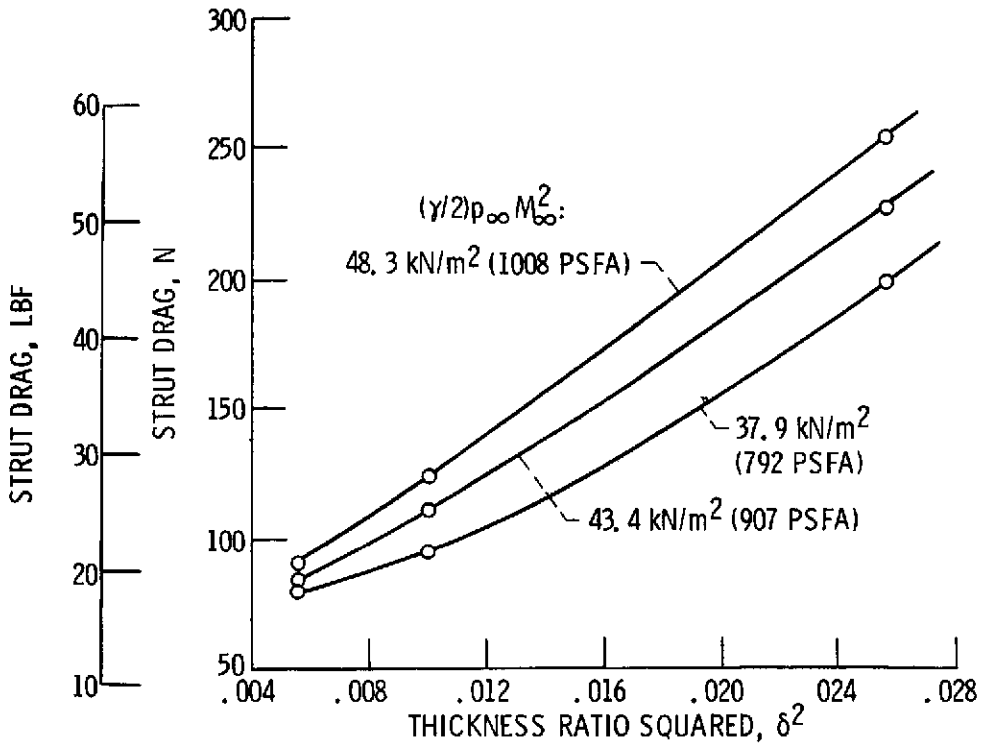

Figure 9. - Experimental strut drag versus thickness ratio squared, Mach 2.5.

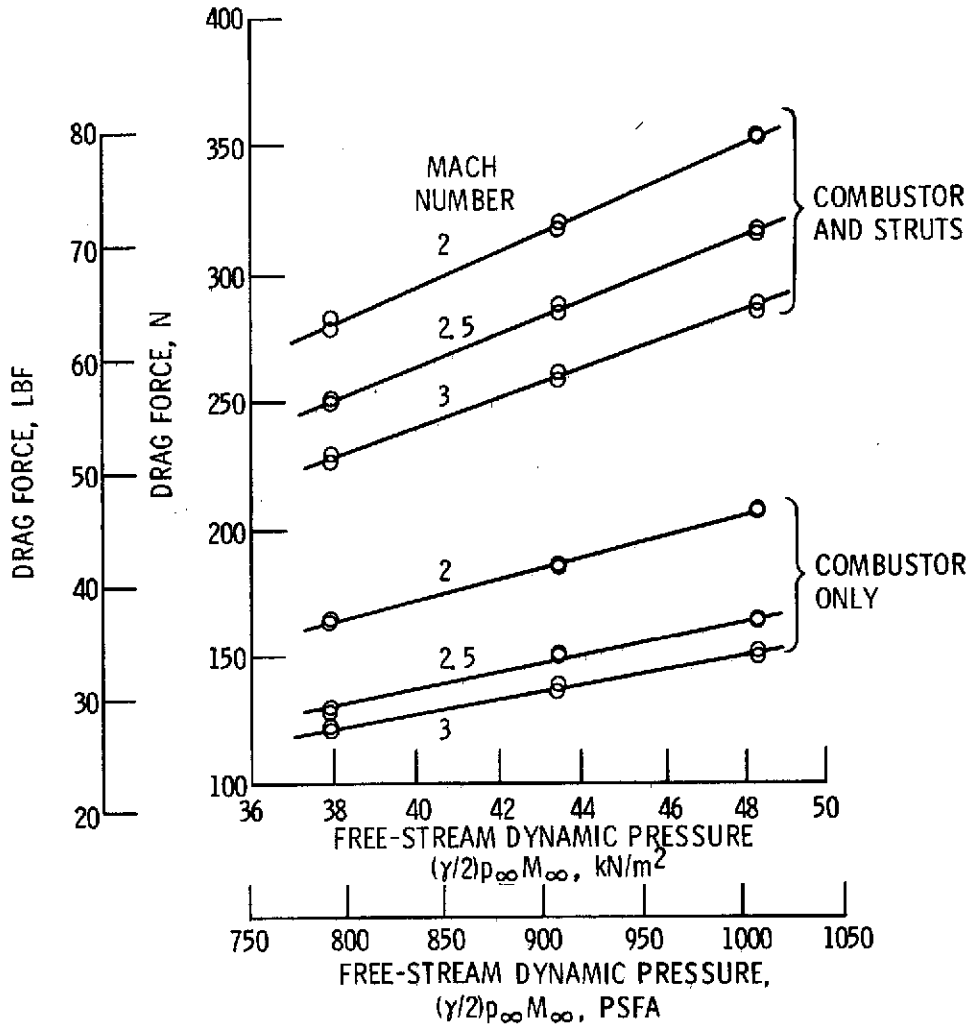

Figure 10. - Experimental drag of strut array (number 7) at various Mach numbers.

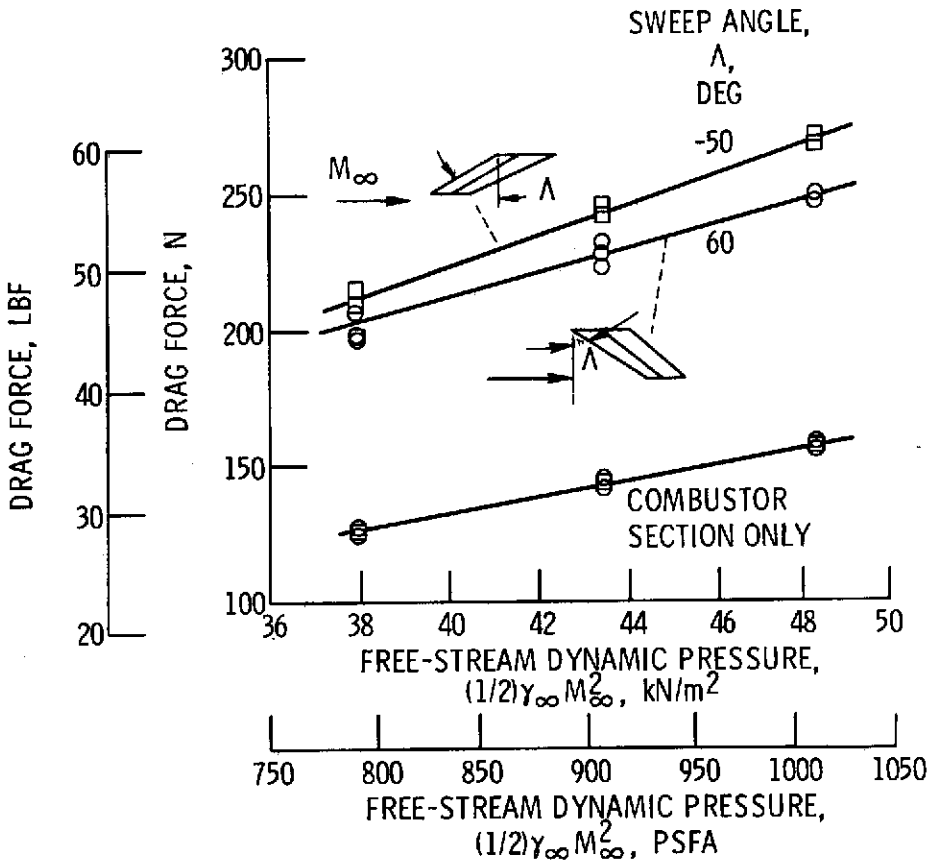

Figure 11. - Effect of sweep back and sweep forward on drag. Mach 2.5; strut number 5.

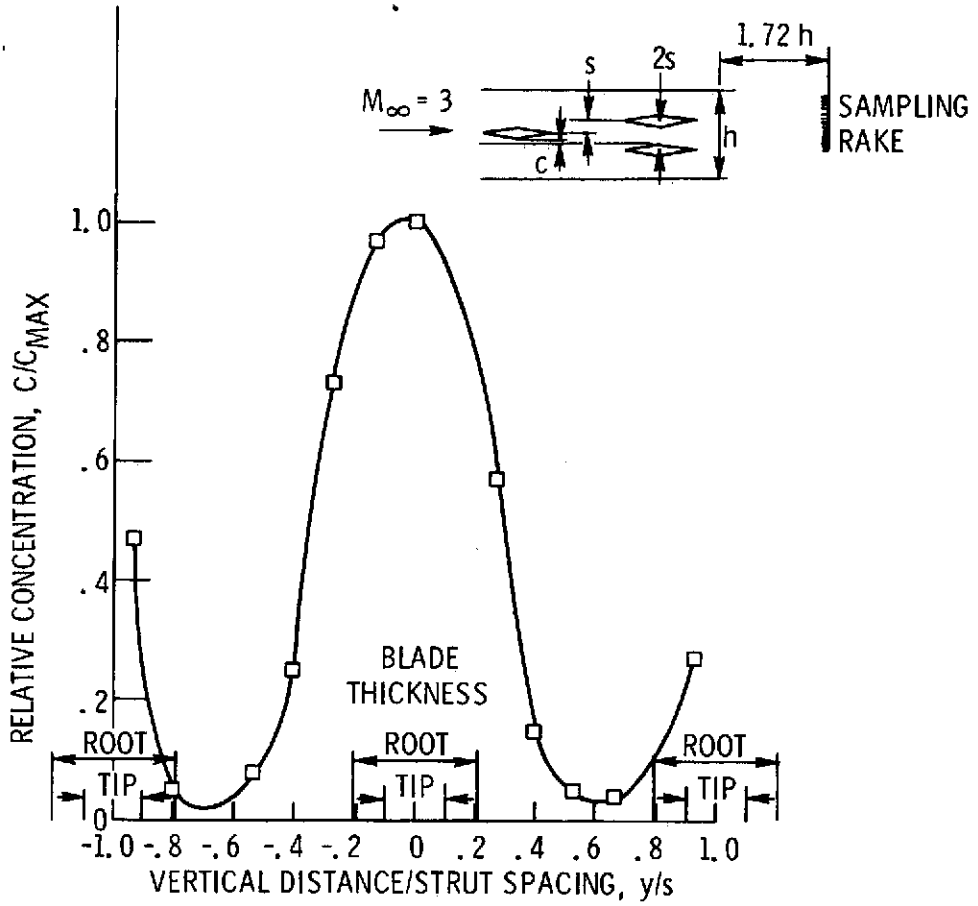

Figure 12. - Helium distribution measurement number 8 struts. Mach 3; z/h, 0.222; He/Air, 0.021.

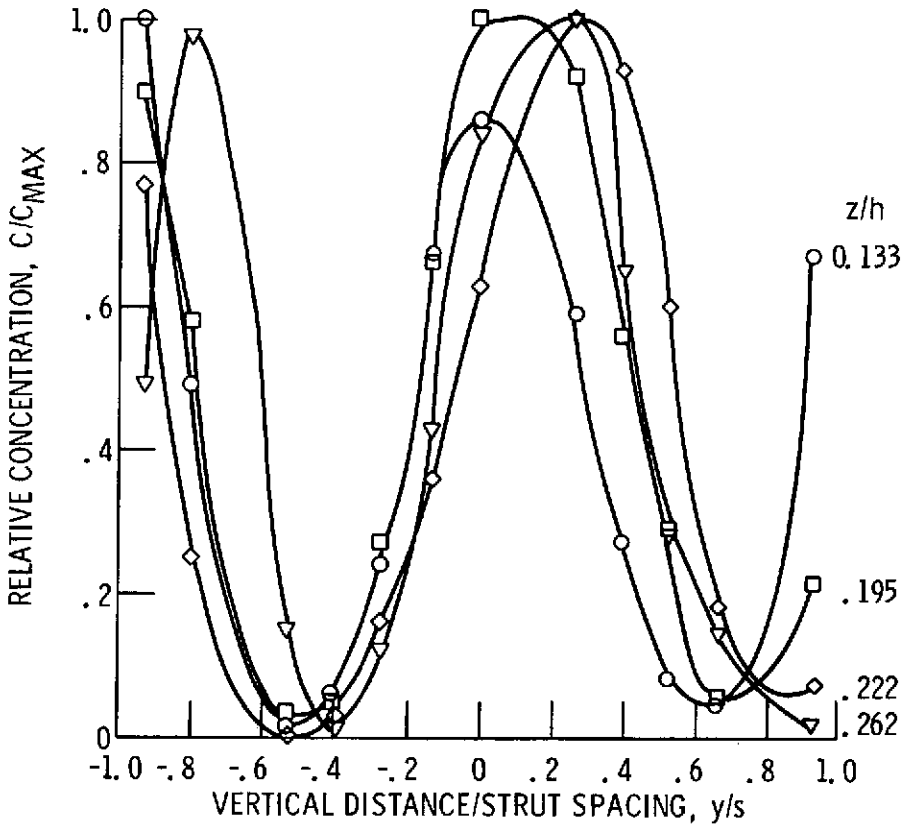

Figure 13. - Helium distribution at various lateral stream positions. Number 5 struts; Mach 3; x/h, 4.50; He/Air, 0.032.

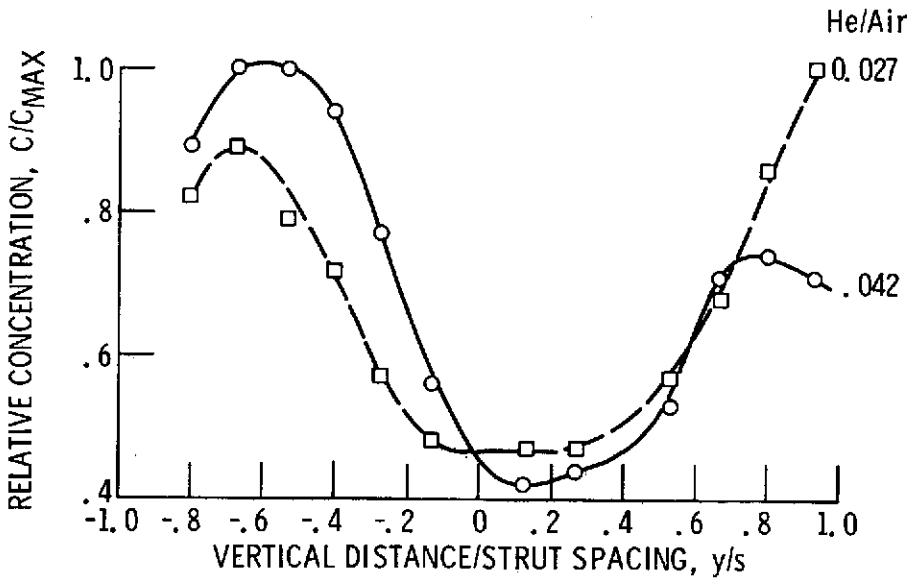

Figure 14. - Helium distribution for variable He/Air ratios. Number 2 struts; Mach 2.5; x/h, 4.50; z/h, 0.222.

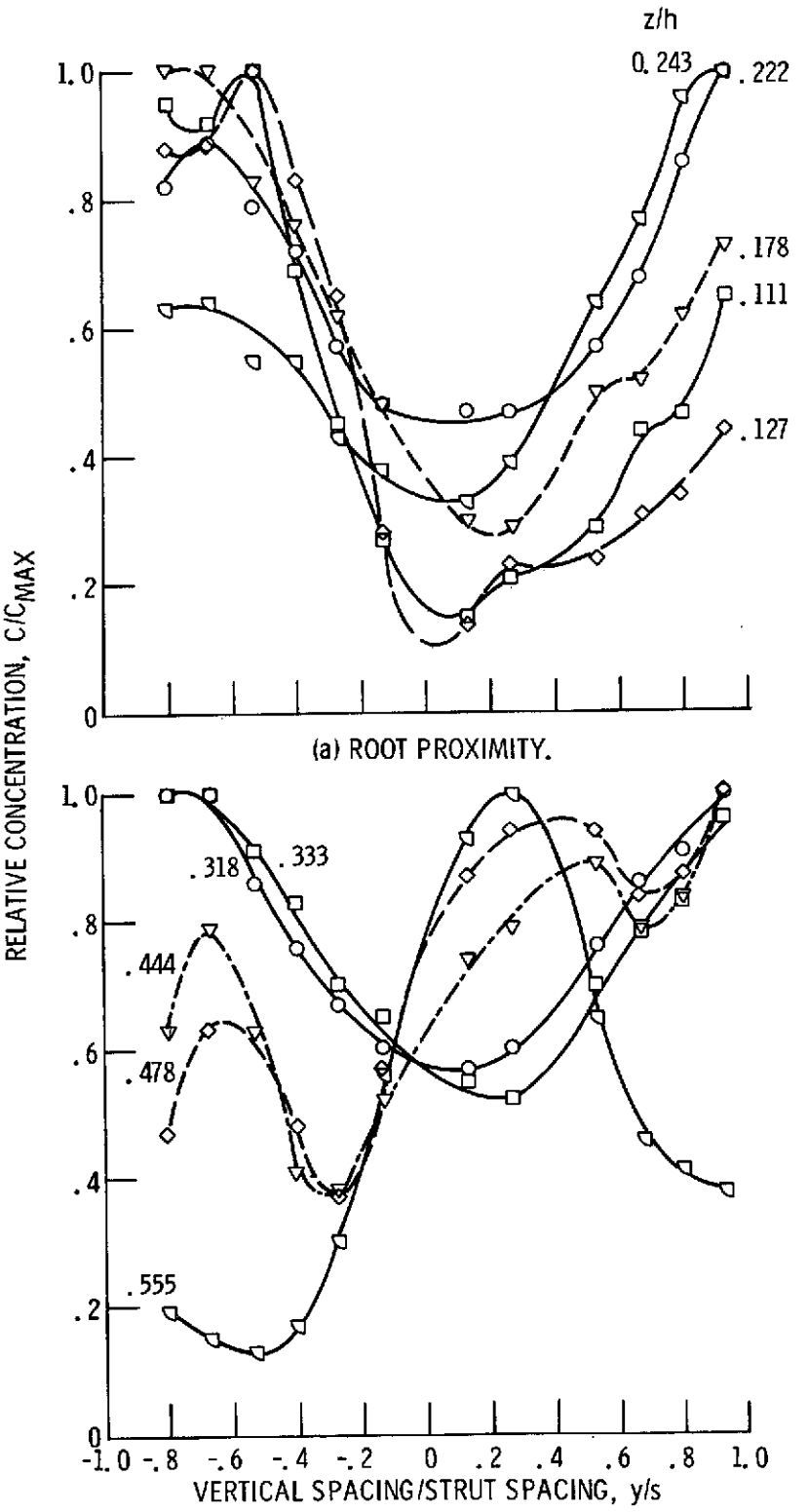

Figure 15. - Helium distribution at various lateral stream positions. Number 2 struts; Mach 2.5, x/h, 4.50; He/Air, 0.027.

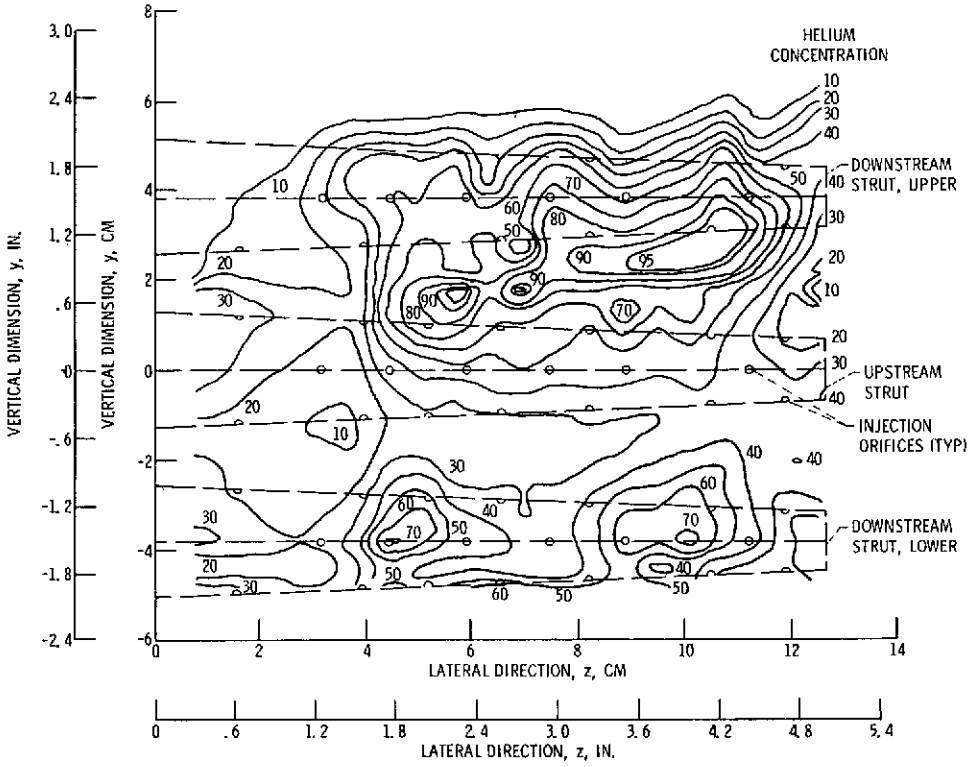

Figure 16. - Helium distribution contours. Number 2 struts; final modification; Mach 2.5; He/Air, 0.031; x/h, 4.50.

NASA-Lewis